Morphology and Properties of Segmented Polyether Polyurethaneureas

Carl B. Wang† and Stuart L. Cooper*

Department of Chemical Engineering, University of Wisconsin, Madison, Wisconsin 53706.
Received June 28, 1982

ABSTRACT: Two series of polyether polyurethaneureas (PEUU) based on 4,4′-methylenebis(phenylene isocyanate), ethylenediamine, and either 1000 or 2000 molecular weight poly(tetramethylene oxide) were synthesized. The effect of the urea linkage, hard segment content, and block length on the extent of phase separation, domain structure, and physical properties was studied by utilizing differential scanning calorimetry, dynamic mechanical, stress–strain, stress hysteresis, and infrared dichroism experiments. The mechanical properties of these polyurethanes depend primarily on the sample's hard segment content, although a higher concentration of urea groups in the PEUU-2000 series results in properties superior to those of the PEUU-1000 series at similar hard segment weight fractions. The presence of three-dimensional hydrogen bonding within hard domains leads to the unusually strong hard domain cohesion. Upon decrease of the hard segment content, a change of morphology from interconnecting to more isolated hard domains took place. Orientation behavior of chain segments within either domain and in the interfacial region is described and related to sample morphology.

Introduction

The unique and novel characteristics of thermoplastic elastomers have recently led to an extensive study of their synthesis, morphology, and properties.[1-4] These materials are formed by joining blocks of two chemically dissimilar segments along the polymer backbone. At service temperature, one of the components is viscous or rubbery (soft segment) while the other is a glassy or semicrystalline thermoplastic (hard segment). The unique properties of these copolymers are directly related to their two-phase microstructure, with the hard domains acting as a reinforcing filler and as a thermally reversible cross-link.

An important class of thermoplastic elastomers is the linear segmented polyurethanes. These polymers have the general structure $(A–B)_n$, where B (the soft segment) is usually formed from a polyether or polyester macroglycol of molecular weight between 600 and 3000. The hard segment is formed by extending a diisocyanate with a low molecular weight diol such as 1,4-butanediol. In the segmented polyurethanes, phase separation of the urethane hard segments into microdomains has been observed even when the segment length is relatively short. The primary driving force for domain formation is the strong intermolecular interaction between the urethane units, which are usually aromatic and capable of forming interurethane hydrogen bonds. Factors that control the degree of microphase separation include copolymer composition, block length, crystallizability of either segment, and the method of sample fabrication. In general, interconnected or isolated hard segment domains are present along with a rubbery phase of soft segment material, though this soft phase may contain some hard segments due to incomplete phase separation. The observation that some of the urethane NH groups form hydrogen bonds with the oxygen of the macroglycol ether or ester linkage[5,6] is consistent with the postulate that some hard segments are dissolved in the soft segment matrix phase.

The incorporation of urea linkages in the polyurethane hard segment has a profound effect on the phase separation and domain structure of polyether polyurethaneureas (PEUU). This is due to the high polarity difference between hard and soft segments and the likely development of a three-dimensional hydrogen-bonding network.[7-9]

In a series of papers by Sung et al.,[8,10,11] the properties of segmented PEUU's based on 2,4-tolyl diisocyanate (2,4-TDI), ethylenediamine (ED), and poly(tetramethylene oxide) (PTMO) have been described. In general, considerable improvement in the extent of microphase separation was found in PEUU's extended with ED compared to all polyurethane systems chain extended with butanediol. This was suggested by a much lower T_g of the soft segment phase and a much higher T_g of the hard segment domains in PEUU's. IR spectra of two PEUU's with 1000 and 2000 molecular weight PTMO were interpreted as consistent with the presence of hard domains containing three-dimensional hydrogen bonding. That is, single urea N–H groups are bonded to two urea carbonyls in a nonplanar three-dimensional configuration. The interface between the hard domain and the soft matrix was suggested to be quite sharp as most of the urethane carbonyls were non hydrogen bonded. In addition, mechanical properties indicated that at the same hard segment content (30%), the hard domains in the PTMO-1000 sample were more interconnected than the hard domains in the PTMO-2000 sample and that the soft segment phase of the former contained more solubilized hard segment.[8]

More recently Wilkes et al.[12] investigated the morphology of Sung's PEUU's using small-angle X-ray scattering and found a consistent interpretation of his data with the results obtained by using mechanical and thermal tests. One important observation was that the one-dimensional correlation function ($\gamma(x)$) displayed periodicity. This suggested that the two-phase microstructure can be described as alternating layers of soft and hard segments whose spacing was given by the calculated periodicity. Wilkes also found that at the same hard segment content, the PTMO-2000 sample showed a higher mean-square fluctuation in electron density ($\langle\rho^2\rangle$) than the PTMO-1000 sample, implying better phase separation. Wilkes suggested that the diamine chain extender promoted better phase separation since the thickness of the interface between the domains in the PEUU's was somewhat less than that of conventional polyurethanes using butanediol as the chain extender.

Ishihara et al.[13] and Kimura et al.[14] studied the deformation mechanism of more crystallizable PEUU's that exhibited spherulitic texture. They recorded as a function of strain IR dichroism, small- and wide-angle X-ray scattering and polarized small-angle light scattering. The

† Present address: IBM Research Laboratories, San Jose, CA.

0024-9297/83/2216-0775$01.50/0

Scheme I
Synthesis of Segmented Polyether Polyurethaneureas[a]

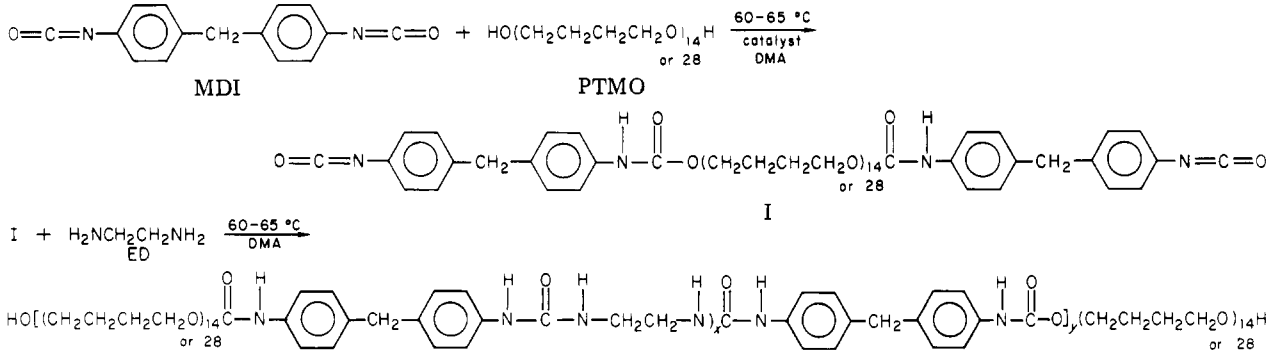

[a] x = 0.3, 1, 1.4, 2, 2.8, or 4.8. DMA = dimethylacetamide.

Table I
Sample Characterization and Number of Specified Groups/Repeat Unit

sample	molar ratio MDI/ED/PTMO	molecular weight of PTMO	hard segment, wt %	ED, wt %	X_B, fraction of bonded urethane carbonyl	functional groups of urethaneurea repeat unit		
						NH	C=O	C=O
PEUU-46-2000	5.8/4.8/1.0	1996	46.5	7.7	0.41	21.2	2	9.6
PEUU-46-1000	3/2/1	1008	46.3	6.4	0.41	10	2	4
PEUU-36-2000	3.8/2.8/1.0	1996	35.9	5.4	0.38	13.2	2	5.6
PEUU-36-1000	2/1/1	1008	35.7	3.8	0.37	6	2	2
PEUU-25-1000	2.4/1.4/1.0	1996	25.5	3.1	0.33	7.6	2	2.8
PEUU-25-2000	1.3/0.3/1.0	1008	25.4	1.3	0.33	3.2	2	0.6

authors observed an inversion or transition from negative to positive IR dichroism for hard segment carbonyl groups. This observation along with X-ray diffraction results suggested a restructuring of the hard segment domains with strain.

In contrast, Khranovskii et al.,[15] in their study of a PEUU composed of 2,4-TDI, bis(4-aminophenyl)methane, and PTMO, interpreted the transverse orientation (at low elongations) as due to a conformational change of the hard segment from a twisted to a more extended form. The hard segment in this polymer contains mostly benzene rings linked by urea groups, which may, because of steric hindrance, lead to the twisted conformation.

Up until the present time, studies of segmented polyether polyurethaneureas made by using MDI, ED, and PTMO (with molecular weight ranging from 500 to 2500) were mostly limited to the molar ratios of 2:1:1.[7,9,13,14] Basically, diisocyanate end-capped macroglycols were chain extended by 1 mol of diamine. Therefore, it was of interest to synthesize a series of PEUU's to investigate how the hard segment content and block length affects morphology and physical properties in these materials. In this study, two series of PEUU's were synthesized having 1000 and 2000 molecular weight PTMOs as the soft segments. Each series of samples contained three levels of hard segment content chosen to maintain comparable hard segment weight fractions between the systems.

Experimental Section

A. Synthesis. Segmented PEUU's were synthesized by a two-step condensation reaction[16] (Scheme I).

4,4'-Methylenebis(phenylene isocyanate) (MDI) (Eastman Kodak Chemical Co.) was vacuum distilled. *N,N'*-Dimethylacetamide (DMA, 99% in purity) (Aldrich Chemical Co.) and PTMO of 1000 and 2000 molecular weight (MW) (Quaker Oats Co.) were dehydrated under vacuum at 45–50 °C for 24 h. ED (99% in purity) (Aldrich Chemical Co.) and stannous octoate (M&T Chemicals) were used as received.

A solution of MDI was prepared in DMA. PTMO and catalyst were subsequently added to the stirred MDI solution at room temperature. The concentration of reactants in solution was about 15% w/v and of the catalyst was 0.4–0.5% by weight of the reactants. After reacting at 60–65 °C for 1 h, the mixture was cooled down to 30 °C, ED added, and the temperature gradually brought back to 60–65 °C. This was to prevent an excessively rapid reaction of the highly reactive aliphatic diamine chain extender. The reaction was continued for an additional hour at about 65 °C. The entire synthesis was performed under a continuous purge of dry N_2. The molar ratio of MDI, ED, and PTMO and the soft segment (PTMO) molecular weight were altered in different syntheses to produce samples with systematically varied hard segment content and block length (Table I).

The polymers were precipitated and dried in a vacuum oven at 70–75 °C for 1 week. Films for physical testing were prepared by spin casting[17] a polymer solution in DMA at 70 °C, followed by vacuum drying at 70 °C for 4 days. A polymer made from 3 mol of MDI, 2 mol of ED, and 1 mol of 1000 MW PTMO is designated as PEUU-46-1000 where the first two digits representing the weight percent hard segment content are followed by the soft segment molecular weight.

B. Experimental Methods. DSC thermograms over the temperature range −120 to 220 °C were recorded by using a Perkin-Elmer DSC-II linked to a Perkin-Elmer Thermal Analysis Data Station. The experiments were carried out at a heating rate of 20 °C/min under a He purge. Sample weights were 20 ± 2 mg. The empty-pan DSC base line was subtracted from each sample's thermogram by means of a scanning autozero module, and the data were further normalized to an equivalent sample weight.

Dynamic mechanical data were collected at 110 Hz at a 2 °C/min heating rate under a N_2 purge with a Toyo Rheovibron DDV-IIC configured for automatic data acquisition. All control and data acquisition were accomplished by using a LSI 11/3-based microprocessor. The temperature-ramping algorithm used derivative control. Prestraining was accomplished with a positioning dc motor and a nonlinear control algorithm. After conditioning the force and displacement transducer, signals were analyzed by a vector voltmeter whose two-channel output is digitized. Test data are displayed, recorded on disk, and plotted by using a Houston Instrument DMP-4 digital plotter.

Uniaxial stress–strain experiments were made with an Instron tensile testing apparatus at room temperature, with a crosshead speed of 0.5 in./min. Samples were cut with an ASTM 412 die and had a gauge length of 1.5 in. The stress was calculated by

Table II
DSC and Rheovibron Data

sample	DSC $T_{g,s}$, °C (onset, end zone width)	DSC ΔC_p at T_g, 10^{-3} mcal/mg s	DSC $T_{c,s}$,[a] °C	DSC $T_{m,s}$,[b] °C	DSC $T_{m,h}$,[e] °C	Vibron E'' (tan δ), °C secondary relaxation	Vibron $T_{g,s}$	Vibron T_h[f]
PEUU-46-1000	−48 (−71, −14, 57)	19.7			291	−129 (−124)	−38 (−23)	(145[g]), 219 (223)
PEUU-46-2000	−75 (−86, −65, 21)	14.8	−48	−4	298	−127 (−127)	−66 (−59)	145 (166)
PEUU-36-1000	−52 (−75, −31, 44)	30.9			292	−126 (−123)	−40 (−20)	
PEUU-36-2000	−74 (−90, −60, 30)	24.0	−53	−2	292	−127 (−129)	−69 (−57)	143 (150), 220 (232)
PEUU-25-1000	−47 (−70, −31, 39)	39.4				−125 (−121)	−40 (−27)	
PEUU-25-2000	−69 (−80, −57, 23)	31.4	−36	9		−131 (−125)	−62 (−53)	(76)
PTMO-1000	−82 (−92, −75, 17)	6.1		24,[c] 37[d]				
PTMO-2000	−79 (−91, −73, 18)	6.6		24,[c] 47[d]				

[a] Soft segment crystallization temperature. [b] Soft segment melting point. [c] Metastable melting point. [d] Equilibrium melting point. [e] Hard segment melting point. [f] Hard segment damping peak. [g] Shoulder.

using the initial cross-sectional area.

Stress hysteresis measurements were made by loading and unloading the specimen at a crosshead speed of 0.5 in./min. These experiments were carried out at increasing strain levels. The percent hysteresis for a given cycle is calculated from the ratio of the area bounded by the loading–unloading curves to the total area under the loading curve.

Survey IR spectra of samples were obtained with a Nicolet 7199 Fourier transform infrared spectrophotometer at a resolution of 4 cm^{-1}. The peak positions for the specific functional groups such as NH and C=O were determined to the nearest 0.5 cm^{-1}.

Infrared dichroism measurements were obtained by coupling the FTIR with a stretching device, which elongated the sample film from both ends simultaneously. The jig was mounted in the path of the front beam at a 90° angle with respect to the laboratory Z axis. A Perkin-Elmer gold-wire grid polarizer was inserted between the sample and detector and set at 90° or 0°, respectively, for recording $A_\parallel$ or $A_\perp$. Five minutes of stress relaxation was allowed before the polarized spectra were recorded. An accumulation of 32 scans was automatically made at each polarizing angle.

The theory and application of infrared dichroism have been well documented elsewhere.[18,19] In multiphase polymer systems, infrared dichroism can be used to study the deformation of chain segments in each domain by following the absorptions of functional groups residing on segments in different phases.

An analysis of the IR peak intensities similar to that of Seymour et al.[20] was performed to determine if any change in the concentration of hydrogen-bonded functional groups with deformation occurs. Assuming cylindrical symmetry, it can be shown that for a uniaxially oriented sample the average absorbance A is given by eq 1. This relation has been used throughout in the calculation

$$A = \tfrac{1}{3}(2A_\perp + A_\parallel) \quad (1)$$

of specific absorbances as it should be independent of the orientation of the absorbing groups.

Results and Discussion

A. Thermal Analysis Figure 1 shows the DSC thermograms of the PEUU samples. The transition temperatures, other thermal characteristics, and comparison to dynamic mechanical test results are summarized in Table II. For PEUU samples with 1000 mol wt PTMO (PEUU-1000) a T_g of −47 to −52 °C was observed, which is substantially higher than that of pure PTMO-1000 (a T_g of −82 °C was detected). This indicates a certain degree of hard and soft segment mixing. In addition microphase separation causes the anchoring of the PTMO segments in the phase boundary, which can also raise T_g due to the restrictions imposed by this junction.[38] The PEUU-2000 series exhibited a much lower T_g of −69 to −75 °C and a melting endotherm characteristic of a crystalline PTMO phase. It appears that in a PEUU-2000 series, hard segments solubilization in the soft segment matrix is minimal.

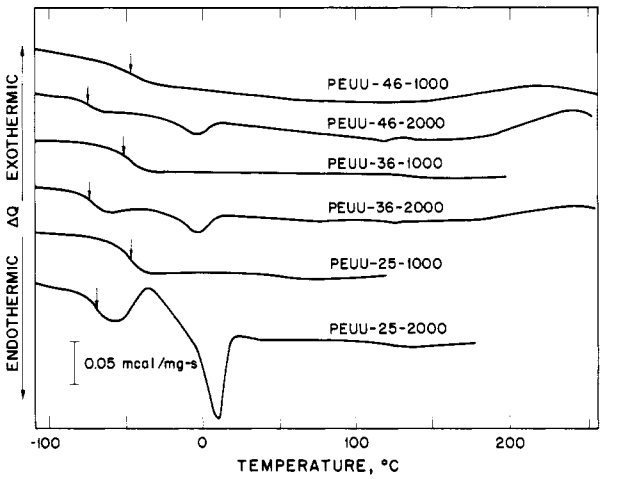

Figure 1. DSC curves of the as-cast polyether polyurethaneurea samples.

Hu et al.[21] have recently presented a rationalization for the degree of phase separation in segmented polyurethaneureas that is related to the crystallizability of the soft segment. In Hu's study as well as in the data presented here the presence of a PTMO melting endotherm in the PEUU-2000 series correlates with improved microphase separation.

It is desirable to characterize the differences in morphology of the two series of PEUU samples. The morphology of the PEUU-2000 series consists of relatively pure hard and soft segment domains with a possible limited interaction between the urethane (and urea) groups and the polyether matrix at the interface. The partially phase mixed morphology of the PEUU-1000 samples is more complicated. Knutson et al.[9] suggest that the morphology may be characterized by segments of polyether dispersed within the hard domains and/or by polyurethaneurea segments dispersed in the polyether matrix. They also described another alternative involving relatively pure polyurethaneurea and polyether domains separated by a rather broad interfacial zone. On the basis of the DSC and IR results (to be discussed later), the morphology of PEUU-1000 probably combines aspects of both models. Because the urea carbonyls in PEUU-1000 were observed to be nearly completely hydrogen bonded, it seems unlikely that individual hard segments are dispersed in the polyether matrix. However, if some hard segments form domains of very small size, those domains could more effectively raise the soft segment T_g.

In Table II, the onset and end temperature of the T_g range and the glass transition zone width (ΔT) are listed. It is noted that at constant hard segment content, the ΔT

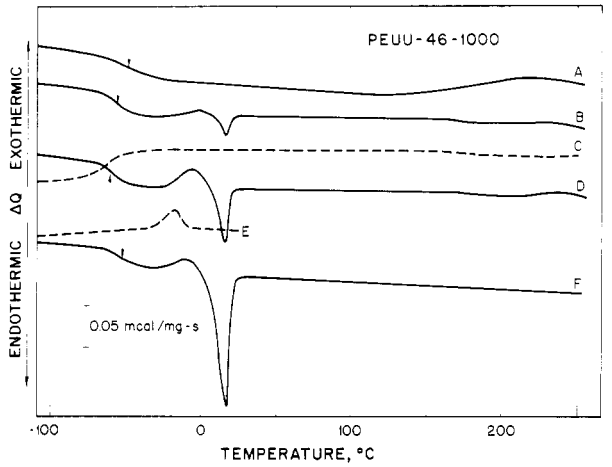

Figure 2. DSC curves of PEUU-46-1000: (A) first heating at 20 °C/min; (B) second heating at 20 °C/min, after quenching from 250 °C; (C) second cooling at −20 °C/min; (D) third heating at 20 °C/min; (E) third cooling at −5 °C/min; (F) fourth heating at 20 °C/min.

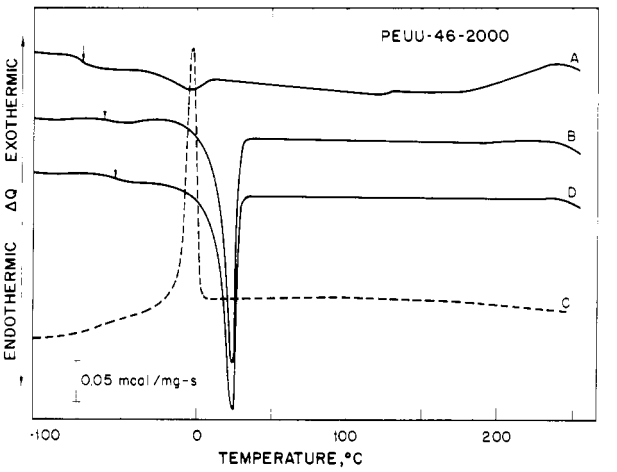

Figure 3. DSC curves of PEUU-46-2000: (A) first heating at 20 °C/min; (B) second heating at 20 °C/min, after quenching from 250 °C; (C) second cooling at −20 °C/min; (D) third heating at 20 °C/min.

of the PEUU-1000 series is approximately 1.5–3.0 times as wide as that of the PEUU-2000 series. This suggests a higher degree of structural heterogeneity in the PEUU-1000 series in which small bundles of hard segments are more or less solubilized in the soft segment phase.

The magnitude of the heat capacity change (ΔC_p) at the soft segment T_g, normalized to the weight of the soft segment, is a function of both the relative amount of the participating amorphous phase and the difference of conformational entropy between the glassy and rubbery state. At constant hard (and soft) segment content, it is observed that ΔC_p of the PEUU-1000 series is about 30% larger than that of the PEUU-2000 series. This is probably caused by the fact that the quantity of amorphous polyether segments in the series PEUU-2000 is reduced because of PTMO crystallization.

In order to study the effect of thermal history on the transitions of the PEUU's, a sequence of in situ thermal treatments was applied to each of the samples. After the original heating curve (Figure 1) had been obtained each sample was (1) quenched from about 200 to −110 °C at −320 °C/min followed by heating at 20 °C/min, (2) cooled from 200 to −110 °C at −20 °C/min followed by heating at 20 °C/min, and (3) cooled from 200 to 27 °C (room temperature) at −20 °C/min and from 27 to −110 °C at −5 °C/min followed by heating. Trial experiments showed that cooling at −5 °C/min throughout the whole temperature range did not create measurable differences in thermal properties compared to the two-step cooling treatment (3 above). DSC data for each sample subjected to the above thermal treatments are summarized in Table III. The percent crystallinity of the soft segment is determined by comparing the areas under the melting peak of the DSC scans, normalized to unit weight of the soft segment. Figure 2 shows the heating (solid line) and cooling (dashed line) DSC scan for PEUU-46-1000, which has the longest hard segment among the PEUU-1000 series. The growth of the PTMO melting endotherm at about 16 °C (Figure 2, curves B, D, and F) suggests that soft segment crystallization proceeds more completely under a slower cooling rate. Cooling curve E also shows a crystallization exotherm. Slow cooling appears to enhance phase separation and soft segment crystallization simultaneously, which explains the observation of a minimum in soft segment T_g (Figure 2, curves B, D, and F, and Table III). T_g dropped initially (−20 °C/min cooling rate) due to more complete microphase separation. However,

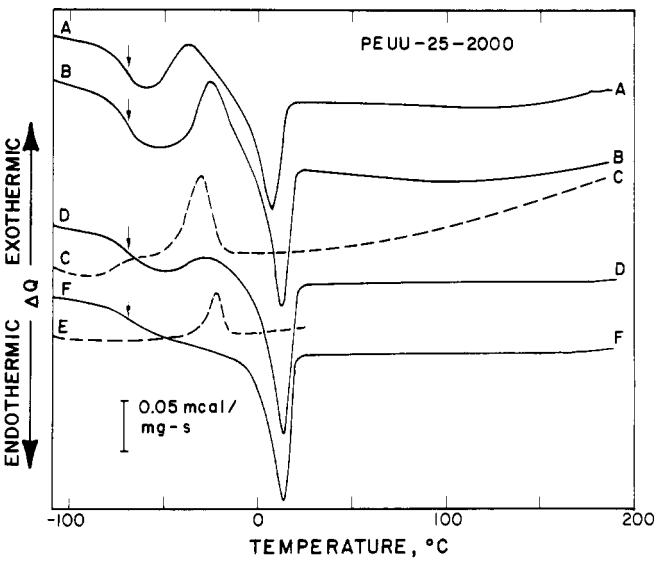

Figure 4. DSC curves of PEUU-25-2000: (A) first heating at 20 °C/min; (B) second heating at 20 °C/min, after quenching from 190 °C; (C) second cooling at −20 °C/min; (D) third heating at 20 °C/min; (E) third cooling at −5 °C/min; (F) fourth heating at 20 °C/min. Arrows denote T_g of polyether domain.

upon cooling under conditions that enchance crystallization substantially (−5 °C/min) the soft segment T_g is raised due to amorphous phase constraints imposed by the higher concentration of PTMO crystallites. The samples PEUU-36-1000 and PEUU-25-1000 were less sensitive to the applied thermal treatments. Figure 3 shows the effect of the thermal history on the transitions of PEUU-46-2000. Similar behavior was also observed for PEUU-36-2000 (not shown). It is noted that both quenching and slow cooling (at −20 °C/min) enhance soft segment crystallization. Table III shows that increasing PTMO crystallization raises the soft segment T_g. Figure 4 shows the DSC scans for PEUU-25-2000. The soft segment in this material is less affected by the hard domains than the two other PEUU-2000 series samples. Thus, relatively large soft segment crystallization and melting peaks are observed. The fact that the various thermal treatments do not affect soft segment crystallinity (Table III) is consistent with the observation of a T_g that is independent of the sample thermal history.

It is interesting to compare the soft segment T_m of the PEUU samples with different thermal histories with that

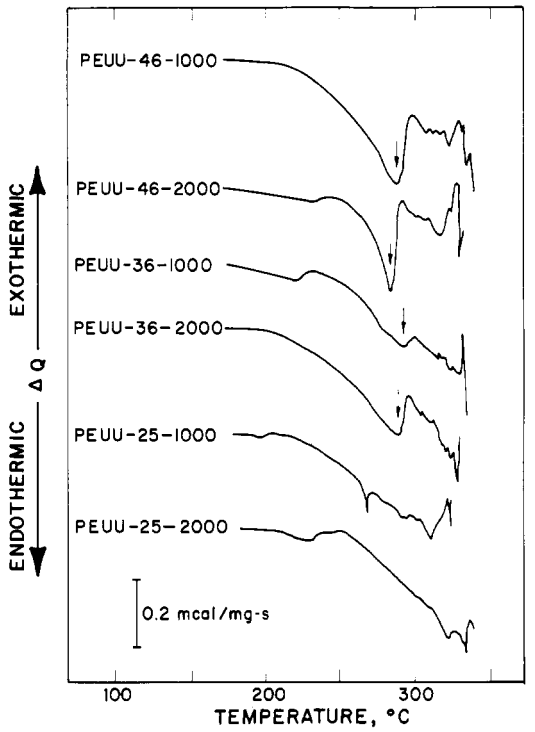

Figure 5. High-temperature DSC curves of the as-cast polyether polyurethaneurea samples. Arrows denote T_m of polyurethaneurea domain.

of the pure PTMO macroglycols. In a copolymer consisting of A units, which crystallize and B units, which do not, if the units occur in a random sequence along the chain, the B units should depress the melting point.[22-24] This classical melting point depression theory is also consistent with experimental results on compatible polymer blends.[25,26] Although PEUU materials in this work are not random copolymers, for samples having hard segments solubilized in soft segment matrix a melting point depression is likely. Table III lists the soft segment T_m estimated by using the minimal point of the corresponding melting endotherm. Both PTMO-1000 and PTMO-2000 exhibited two partially overlapping melting peaks (DSC scans not shown). The low-temperature endotherm is attributed to the melting of metastable PTMO crystallites. The higher temperature melting peak is associated with crystalline PTMO segments closer to their equilibrium state. These larger crystals are due to the nearly ideal annealing conditions that room temperature storage affords. Both the thermally cycled PEUU-46-2000 and PEUU-36-2000 showed T_m's similar to that of the low-temperature T_m of PTMO-2000 (Table III). This suggests a high degree of purity within the soft segment matrix after the melt cycling (the first heating is on a solvent-cast sample). The T_m of the cycled PEUU-46-1000 was about 8 °C lower than that of the low-temperature T_m of PTMO-1000, suggesting some incorporation of solubilized hard segments that depress the melting point. It should also be noted that, while PEUU-25-2000 contained a well-phase-separated morphology, the soft segment T_g was higher and the T_m was lower than that of the other two PEUU-2000 materials. This is probably due to the relatively short hard segment length (and content) in PEUU-25-2000, which causes partial hard to soft segment intermixing as well as an isolated hard segment domain morphology (to be discussed later).

Separate high-temperature DSC experiments were carried out on the as-cast samples, in order to characterize hard segment melting. The results showed a melting endotherm at about 290 °C immediately before reaching the decomposition temperature for samples with high (46%) and medium (36%) hard segment content. The DSC curves from 180 to 350 °C are depicted in Figure 5 and the averaged T_m (out of 4–5 samples) is summarized in Table I. A clear high-temperature melting endotherm was not observable in the polyurethaneureas containing 25 wt % hard segment. Compared to the diol-extended polyether–urethanes the crystalline hard domains of the PEUU's seem to introduce superior mechanical properties and high-temperature performance. Details will be described in the sections on mechanical properties.

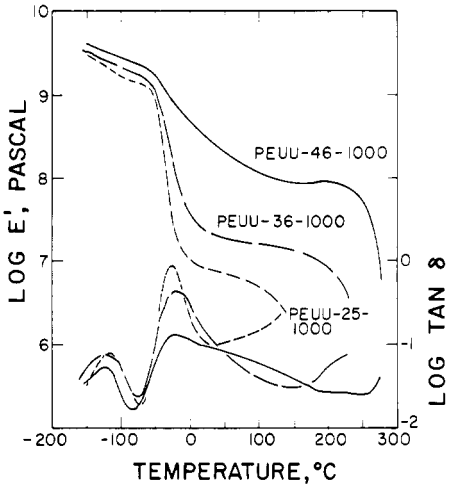

Figure 6. Storage modulus E' and tan δ curves of the PEUU-1000 series: (—) PEUU-46-1000; (– –) PEUU-36-1000; (- - -) PEUU-25-1000.

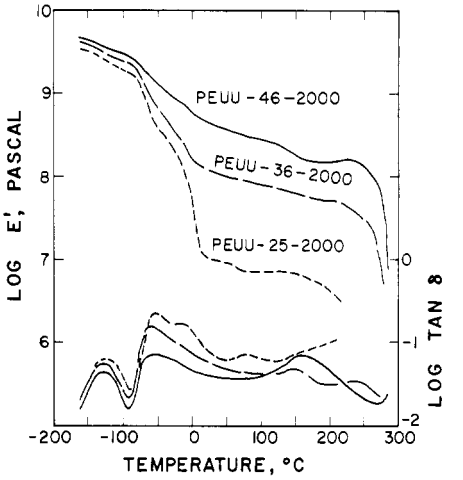

Figure 7. Storage modulus and tan δ curves of the PEUU-2000 series: (—) PEUU-46-2000; (– –) PEUU-36-2000; (- - -) PEUU-25-2000.

B. Dynamic Mechanical Properties. The storage modulus (E') and the dissipation factor (tan δ) of the PEUU-1000 series and the PEUU-2000 series are plotted as a function of temperature in Figures 6 and 7, respectively. Peak positions in the tan δ and E'' curves (the loss modulus curves not shown) are summarized in Table II. Despite the variation in sample composition and block length, two maxima in the tan δ curve occur at approximately −125 and −25 °C (for the PEUU-1000 series) or −58 °C (for the PEUU-2000 series). The low-temperature loss peak is related to the local mode motion of the $(-CH_2-)_4O$ group,[27] whereas the high-temperature loss peak is attributed to the backbone motion of soft segment that accompanies its glass transition. Several high-temperature damping peaks (or shoulders) relating to the hard segment

Table III
DSC Results of PEUU's under Various Thermal Treatments

sample	thermal condition[a]	T_g (zone width), °C	$T_{c,s}$, °C	$T_{m,s}$, °C	soft segment: heat of fusion,[d] mcal/mg	soft segment: % crystallinity[f]
PEUU-46-1000	1st heating	−48 (60)				
	2nd heating after quenching	−55 (29)	−4	16	0.8	1.5
	2nd cooling[b]	−63 (31)				
	3rd heating	−60 (37)	−8	15	2.6	5.0
	3rd cooling[c]		−18			
	4th heating	−52 (37)	−11	16	8.8	16.6
PEUU-46-2000	1st heating	−75 (21)	−48	−5	1.8	3.4
	2nd heating after quenching	−61 (21)	−22	24	15.9	29.9
	2nd cooling[c]		−2			
	3rd heating	−54 (26)		24	16.7	31.4
PEUU-36-1000	1st heating	−52 (44)				
	2nd heating after quenching	−52 (42)				
	2nd cooling[b]	−58 (46)				
	3rd heating	−52 (41)				
	3rd cooling[c]	−58 (18)				
	4th heating	−54 (41)				
PEUU-36-2000	1st heating	−74 (30)	−41	−1	1.7	3.2
	2nd heating after quenching	−59 (28)	−28	24	16.8	31.8
	2nd cooling[b]		1			
	3rd heating	−56 (46)		25	17.9	33.8
PEUU-25-1000	1st heating	−47 (39)				
	2nd heating after quenching	−48 (34)				
	2nd cooling[b]	−55 (31)				
	3rd heating	−48 (30)				
	3rd cooling[c]	−54 (17)				
PEUU-25-2000	1st heating	−71 (22)	−37	7	4.5	8.5
	2nd heating after quenching	−70 (29)	−25	13	4.9	9.3
	2nd cooling[b]	−77	−30			
	2rd heating	−68 (31)	−27	14	5.9	11.1
	3rd cooling[c]		−23			
	4th heating	−68 (31)		13	5.5	10.4
PTMO-1000	1st heating	−82 (18)		−24, 37	23.1[e]	43.6
	2nd heating after quenching	−82 (20)		24	22.9	43.1
	2nd cooling[b]		−1			
	3rd heating	−84 (22)		24	22.4	42.3
	3rd cooling[c]		6			
	4th heating	−83 (22)		23	23.8	44.9
PTMO-2000	1st heating	−79 (21)		24, 47	29.2[e]	55.1
	2nd heating after quenching	−80 (21)		28	23.4	44.2
	2nd cooling[b]		−1			
	3rd heating	−80 (23)		28	22.2	42.0
	3rd cooling[c]		7			
	4th heating	−79 (22)		28	23.1	43.5

[a] Heating rate was maintained at 20 °C/min throughout the experiment. [b] Cooling rate was −20 °C/min. [c] Cooling rate was −20 °C/min from about 200 to 27 °C followed by −5 °C/min to −110 °C. [d] Calculated based on 1 mg of soft segment. [e] Total heat of fusion assuming little difference in molar heat of fusion between the metastable state and the equilibrium state. [f] Calculated by using a heat of fusion for 100% crystalling poly(tetramethylene oxide) of 53.0 mcal/mg.[22]

domains in some of the PEUU materials were also detected.

The E' results indicate that all of the samples except PEUU-25-1000 exhibited a rubbery plateau that extended beyond 200 °C. The plateau modulus increases upon increasing the hard segment content in the samples. Comparison of the PEUU-2000 series with the PEUU-1000 series of the same hard segment content reveals a higher plateau modulus in the former. It is well-known that the thermoplastic polyurethane elastomers are self-reinforced by the hard segment domains, which are phase separated from the polyether (or polyester) matrix. Substitution of a diamine chain extender in place of the usual diol creates not only a larger soft/hard segment polarity difference but also semicrystalline hard domains of unusually high T_m. This results in better phase separation and an enhanced physical cross-linking and/or filler effect. The PEUU-2000 series have a higher volume fraction of "effective" filler due to the more complete phase separation in these polymers. In addition to the longer hard segments, PEUU-2000 polymers also have a higher concentration of urea groups (Table I) whose hydrogen-bonding network enhances intradomain cohesion. Furthermore, the more cohesive hard segments in PEUU materials impart higher hard segment melting points and thus higher short-term thermal stability as compared to the polyether polyurethanes of similar hard segment content.

C. Tensile Properties. The tensile behavior of thermoplastic elastomers generally depends on the size, shape, and concentration of the hard domains,[28,29] intermolecular bonding within the hard domains, and the ability of the soft segment to crystallize under strain. The stress–strain curves of the PEUU samples are shown in Figure 8. Table IV summarizes the tensile properties of the materials studied including Young's and secant moduli, elongation, and stress at failure (ultimate tensile strength).

For all of the samples, an increase of either the hard segment content (at constant soft segment molecular weight) or the block length (at constant hard segment content) leads to a higher Young's modulus and to higher

Table IV
Tensile Properties of Polyether Polyurethaneureas[a]

sample	elongation at failure, %	ultimate tensile strength, 10^6 Pa	Secant modulus, 10^6 Pa 100%	200%	300%	Young's modulus, 10^6 Pa
PEUU-46-2000	570	38.8	13.6	17.6	22.3	188.5
PEUU-46-1000	600	43.0	11.1	15.1	20.3	69.2
PEUU-36-2000	770	40.1	6.9	9.3	12.3	42.6
PEUU-36-1000	850	34.6	4.2	5.8	7.4	9.3
PEUU-25-2000	1160	18.6	2.4	3.3	4.2	4.3
PEUU-25-1000	1550	7.1	1.3	1.7	1.9	3.3

[a] Average data *from* 4-5 tests.

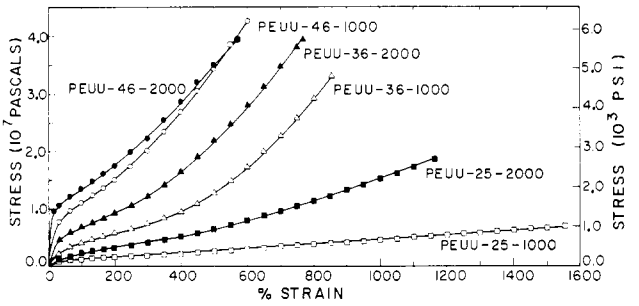

Figure 8. Stress–strain curves for the polyether polyurethaneurea samples.

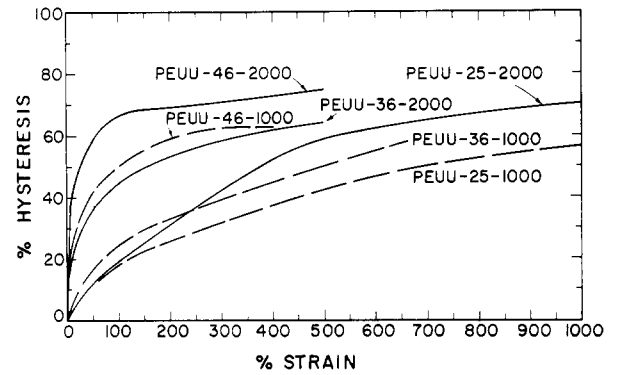

Figure 9. Stress hysteresis vs. elongation curves for the polyether polyurethaneurea samples.

secant moduli. Except for samples of PEUU-46-1000 and PEUU-46-2000, the ultimate tensile strength exhibited the same trend. These results are consistent with the dynamic mechanical data and arise from the introduction of higher volume fractions as well as a higher degree of order in the hard segment domains. The higher modulus and tensile strength of the PEUU-2000 series is consistent with their higher urea content, which results in more cohesive hard domains.

D. Tensile Stress Hysteresis Studies. In a multiphase system, the stress hysteresis behavior is closely related to the domain morphology and phase composition.[8,30,31] A high level of hysteresis at small strains can result from plastic deformation of semicrystalline or glassy structure within the material and/or the disruption of interconnected hard segment domains.

Figure 9 shows that PEUU-46-1000, PEUU-46-2000, and PEUU-36-2000 have higher initial hysteresis than the rest of the PEUU samples. It appears that a combination of hard domain interconnectivity and a higher degree of order in the hard domains of these samples causes the plastic deformation to occur at lower strains and to a greater extent compared to samples of lower hard segment content. PEUU-36-1000 and PEUU-25-1000 show more rubbery behavior with a relatively high recovery, suggestive of a morphology consisting of isolated hard domains dispersed in an amorphous soft segment matrix. Although PEUU-25-2000 resides initially in the family of low hysteresis, it exhibits a rising rate of hysteresis with increasing strain level. This could be due to the disruption of soft segment crystallinity and the possibility of some irreversible strain-induced crystallization in this sample.

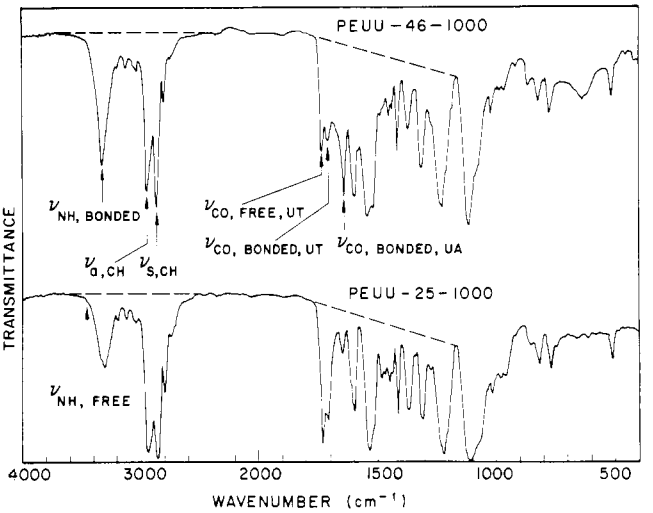

Figure 10. Infrared survey spectrum of PEUU-46-1000 and PEUU-25-1000.

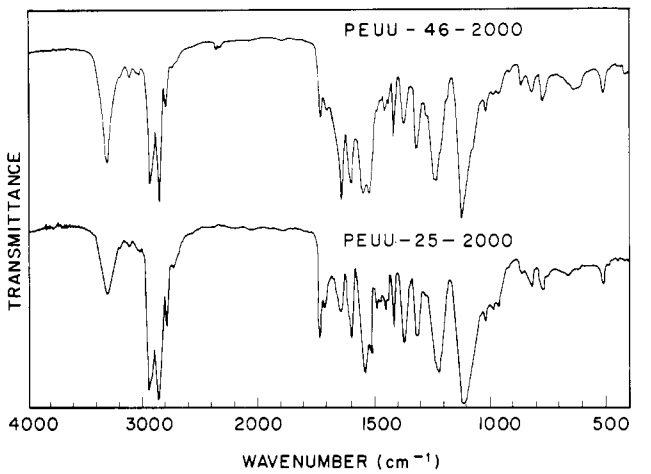

Figure 11. Infrared survey spectrum of PEUU-46-2000 and PEUU-25-2000.

E. Infrared Studies. (1) Spectroscopic Analysis. The IR survey spectra of the PEUU samples are shown in Figures 10 and 11. The labeling of several important bands is shown for sample PEUU-46-1000. The spectra are all qualitatively similar. However, as expected, deviations in peak position and relative peak intensity of certain IR bands can be observed among the samples that were synthesized from nearly identical reactants of varying molar ratios.

The NH absorption (peak located between 3305 and 3320 cm^{-1}) is nearly completely hydrogen bonded for all

the samples except PEUU-25-1000, which shows a small shoulder at about 3445 cm^{-1} characteristic of the non-hydrogen-bonded NH groups. In the carbonyl region between 1620 and 1750 cm,$^{-1}$ the peak at 1731~1732 cm^{-1} is due to free urethane carbonyl ($CO_{F,UT}$), the peak at 1705~1710 cm^{-1} is the hydrogen bonded urethane carbonyl ($CO_{B,UT}$), and the band located at 1635~1645 cm^{-1} is the hydrogen-bonded urea carbonyl ($CO_{B,UA}$). A free urea carbonyl peak at 1695 cm^{-1} is not detected.[13] For each sample, the absorbance of NH_B, CO_{UT} (including hydrogen-bonded and free groups), and $CO_{B,UA}$ reflects the relative concentration of these functional groups as summarized in Table I.

In the PEUU's the urethane carbonyls are located only at the junction between the hard and soft segment. The CO_{UT} residing in the small hard segment microdomains solubilized in the polyether matrix phase (e.g., in samples PEUU-36-1000 and PEUU-25-1000) are likely non hydrogen bonded while those located at the interfacial zone between hard domains and soft matrix could be hydrogen bonded or free, depending on the configuration of these groups relative to the nearby NH proton donors.

The relative absorbances of the two urethane carbonyl peaks can serve as an index of the degree to which this group participates in hydrogen bonding. The fraction of hydrogen bonding may be expressed as

$$X_B = \frac{C_B}{C_F + C_B} = \frac{A_B/\epsilon_B}{(A_F/\epsilon_F) + (A_B/\epsilon_B)}$$

where A, C, and ϵ are respectively the absorbance, concentration, and extinction coefficient of bonded (B) and free (F) carbonyl groups. In an earlier study, Spencer et al.[33] measured the free and bonded carbonyl extinction coefficients for polyether polyurethanes and found that ϵ_B/ϵ_F was approximately 1.2. By use of this ratio of extinction coefficients values X_B were calculated and are listed in Table I for the PEUU's studied.

In the PEUU-2000 series, the fraction of bonded urethane carbonyls (Table I) increases upon increasing the hard segment content, suggesting an increase in hard domain ordering. In the PEUU-1000 series, an increase of hard segment content also results in a higher fraction of hydrogen-bonded urethane carbonyls (Table I), as more hard segment ordering occurs and less hard segment microdomains of very small size are dispersed in the polyether matrix phase.

(2) Infrared Spectrum Peak Positions. If there are acid–base or other interactions between chemical groups on either the same or different molecules, the IR peak positions of the participating groups should shift to reflect this interaction. Such interactions are commonly observed in macromolecular systems, and example of which involves hydrogen bonding as already discussed or the behavior of compatible blends in which special interactions promote phase mixing.[34] In the PEUU's of this study the peak positions of NH_B, $CO_{F,UT}$, $CO_{B,UT}$, and $CO_{B,UA}$ were measured as a function of sample composition and block length. Average data from four to five FTIR measurements (one FTIR test accumulated 32 scans) for the above functional groups are depicted in Figure 12. For all of the samples, the $CO_{F,UT}$ absorption stays within a range of 1 cm^{-1}, indicating that the local environment around these urethane carbonyls does not change with sample composition. The $CO_{B,UT}$ groups shifts slightly to lower frequency.

In early studies, Bonart et al.[7] and Sung et al.[8] suggested a three-dimensional hydrogen bond for both MDI- and TDI-based PEUU's where each urea carbonyl was bonded

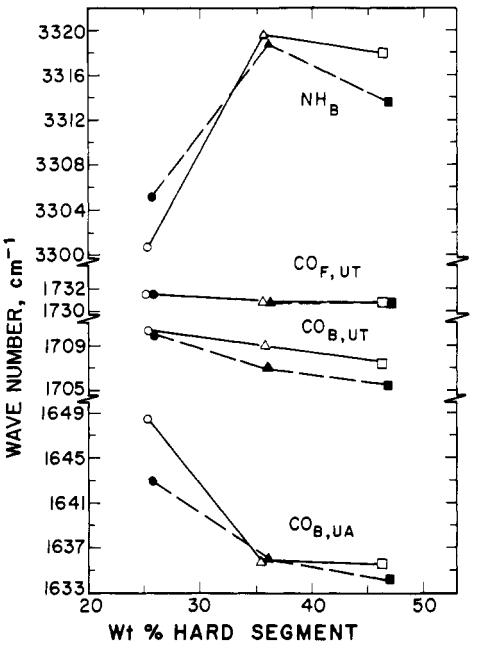

Figure 12. Infrared peak positions of the PEUU-1000 series and PEUU-2000 series (NH_B, $CO_{F,UT}$, $CO_{B,UT}$, and $CO_{B,UA}$: Open symbols, 1000 series; closed symbols, 2000 series.

to two NH groups. It may be expected that between the participating groups, the C=O is affected more than the NH group by the formation of a three-dimensional hydrogen bond. The basis of comparison would be the same groups forming a conventional hydrogen bond where one C=O is bound to one NH group. Overall, the bonded urea C=O should absorb at a lower frequency and the bonded urea NH should absorb at a higher frequency when both groups participate in a three-dimensional hydrogen bond compared to when they form a conventional hydrogen bond. The PEUU-46 and PEUU-36 samples have mostly three-dimensional interurea hydrogen bonding; however, a decrease in hard segment content or, equivalently, an increase in soft segment content results in some soft segments dispersed in the hard domains. This interferes with the ordering of the hard segments and also allows the polyether oxygens to compete with urea carbonyls for the urea NH groups. Both factors result in a mixed state having three-dimensional as well as conventional interurea bonds in samples PEUU-25-1000 and PEUU-25-2000. Thus one observes a large shift in average urea carbonyl peak position to lower frequency upon going from samples containing 25 wt % hard segment to 36 wt %. Although only a fraction of the NH_B groups are involved in interurea hydrogen bonding, a corresponding increase in average NH_B absorption frequency is also noticed.

A similar frequency shift of the urea carbonyl band from 1660 to 1640 cm^{-1} upon going from TDI-based PEUU samples containing 47 wt % hard segment to those containing 53 wt % hard segment has been reported previously[8] and attributed to an increased extent of three-dimensional hydrogen bonding.

(3) Infrared Absorbance vs. Strain. An analysis of IR absorption as a function of strain similar to that of Tanaka et al.[35] and Seymour et al.[20] was performed to determine if any change could be observed in the concentration of NH_B, $CO_{F,UT}$, $CO_{B,UT}$, and $CO_{B,UA}$ groups during sample deformation. The absorbance of each functional group was normalized for changing sample thickness by using the absorbance separately of the asymmetric (at 2940 cm^{-1}) and symmetric (at 2860 cm^{-1}) CH stretching vibrations. To improve the precision of the

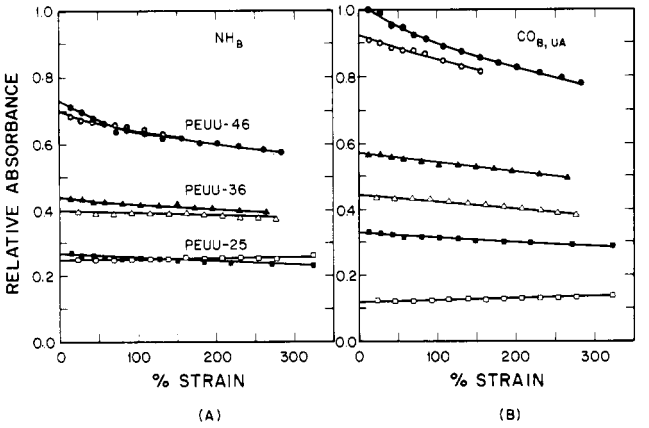

Figure 13. Normalized infrared absorbance vs. elongation curves (A) NH_B and (B) $CO_{B,UA}$ of the polyether polyurethaneurea samples: (○) PEUU-46-1000, (●) PEUU-46-2000, (△) PEUU-36-1000, (▲) PEUU-36-2000, (□) PEUU-25-1000, (■) PEUU-25-2000.

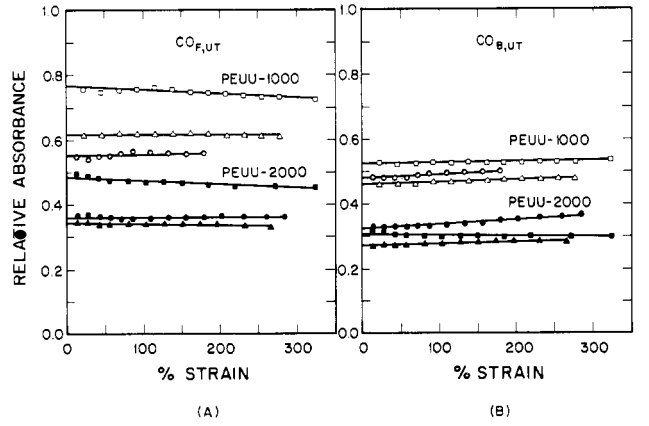

Figure 14. Normalized infrared absorbance vs. elongation curves of (A) $CO_{F,UA}$ and (B) $CO_{B,UT}$ of the polyether polyurethaneurea samples: (○) PEUU-46-1000, (●) PEUU-46-2000, (△) PEUU-36-1000, (▲) PEUU-36-2000, (□) PEUU-25-1000, (■) PEUU-25-2000.

data, both normalized absorptions were calculated and averaged for each of the NH and carbonyl groups studied. Figures 13 and 14 illustrate the relationship between the normalized absorbance (A_N) and the applied strain, with data averaged from five experiments. For each functional group, the magnitude of its absorption in each of the PEUU samples agrees qualitatively with its normalized concentration calculated from the sample's stoichiometry. Figure 13B shows that except for PEUU-25-1000, the concentration of $CO_{B,UA}$ decreased as the sample was elongated. Furthermore, $(A_N)_{CO_{B,UA}}$ decreased at a faster rate for samples of higher hard segment content and block length. The interconnected hard domains in these samples appear to be subjected to the external stress immediately upon sample deformation. This stress disrupts the ordering in the hard domains, possibly leading to dissociation of some of the interurea hydrogen bonding. This is consistent with the stress hysteresis data that indicated that samples of higher hard segment concentration and longer block underwent greater plastic deformation during strain cycling. The NH_B absorption contains contributions from NH groups participating in either interurea, interurethane, or hard to soft segment hydrogen bonding. Thus while the change in $(A_N)_{NH_B}$ with strain is similar to that of the urea carbonyl, it decreases to a lesser extent (Figure 13A). In contrast to the bonded NH and urea carbonyl, both the urethane carbonyl absorptions remain relatively constant upon deformation (Figure 14A,B).

The above results are different from Seymour's observations[20] that stretching up to 300% appears to have little effect on the overall extent of polyurethane hydrogen bonding. Seymour suggested that either very few hydrogen bonds are disrupted when the sample is extended or, alternatively, hydrogen bonds may be disrupted but reformed on a time scale much shorter than that of the experiment. The different behavior of PEUU samples probably originates from the presence of the three-dimensional hydrogen-bonding network in their hard domains. Once sample deformation is initiated, plastic deformation of the hard domains leads to disruption of some of the interurea hydrogen bonds. It appears that the three-dimensional interurea hydrogen bonds may not be re-formed within the time scale of the experiment due to the difficulty of their resuming the proper spatial configuration. The same limitation apparently does not apply in all the polyurethane systems that have the 1:1 type of hydrogen bond.

In an earlier study of polyurethaneureas, Ishihara et al.[13] reported strain-induced changes in the extent of hydrogen bonding on one elastomer. This sample was synthesized by using MDI, ED, and PTMO in molar ratios of 2:1:1. The soft segment had a molecular weight of 1300. They concluded that there was a small decrease of interurethane hydrogen bonding with elongation. No change in the extent of hydrogen bonding in the urea group was observed up to about 50% strain. An abrupt decrease in the interurea hydrogen bonding was reported to occur at 100% strain, which was followed by only a slight decrease in bonding at still higher elongations. Ishihara did not explain why the behavior of NH_B did not parallel that of the $CO_{B,UA}$. Figures 13 and 14 show that PEUU samples of medium (36%) or low (25%) hard segment content behave somewhat differently than Ishihara's sample, which contained 30 wt % hard segments. This may be attributed partly to the difference in morphology since Ishihara studied a material of different soft segment block length. His sample was also prepared by using dimethylformamide (DMF), compared to the materials of this work, which were cast from DMA.

F. Infrared Dichroism. (1) Orientation Characteristics of Polyether Polyurethaneureas. Several functional groups were used to follow segmental orientation in the soft and hard segment domains of the PEUU samples of this study. They include (1) the average behavior of the symmetric and asymmetric CH stretching bands, which are a measure of soft segment orientation, (2) the C=O bond at 1731 cm^{-1}, which is a measure of the average orientation of the non-hydrogen-bonded urethanes either at the hard domain interfacial zone or of hard segments solubilized in the polyether matrix, (3) the C=O absorption band at ~1708 cm^{-1}, which follows the orientation of hydrogen-bonded urethane at the interface, (4) the C=O band at ~1635 cm^{-1}, which is a measure of the orientation of urea linkages within the hard domains, and (5) the NH band at ~3317 cm^{-1}, which characterizes the average hard segment orientation. The transition moment vectors of the CH, C=O, and NH functional gorups were assumed to be respectively 90°, 78°, and 90° to the chain axis.

For simplicity in data manipulation, straight base lines were assumed (3860–2240 cm^{-1} for NH and CH groups, 1800–1170 cm^{-1} for CO groups) and the corresponding peak height was taken to represent the specific polarized infrared absorbance. Dashed lines are drawn in Figure 10 to show how the base lines were constructed; the data were actually obtained from IR absorbance spectra, however. Since all of the FTIR spectra for the PEUU samples were

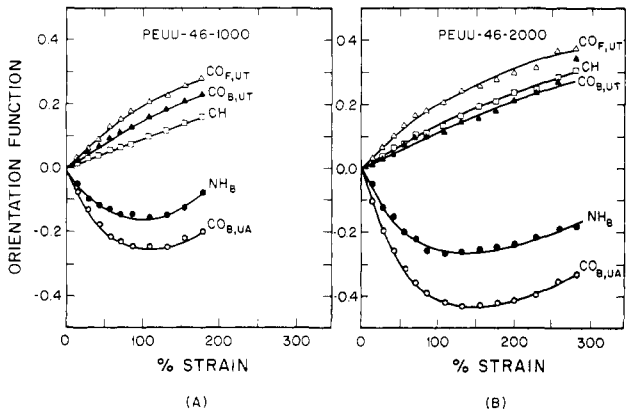

Figure 15. Orientation function vs. elongation curves of (A) PEUU-46-1000 and (B) PEUU-46-2000: (□) CH, (△) $CO_{F,UT}$, (▲) $CO_{B,UT}$, (●) NH_B, (○) $CO_{B,UA}$.

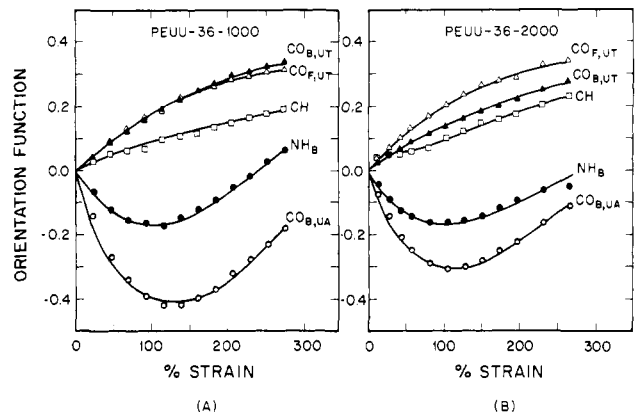

Figure 16. orientation function vs. elongation curves of (A) PEUU-36-1000 and (B) PEUU-36-2000: (□) CH, (△) $CO_{F,UT}$, (▲) $CO_{B,UT}$, (●) NH_B, (○) $CO_{B,UA}$.

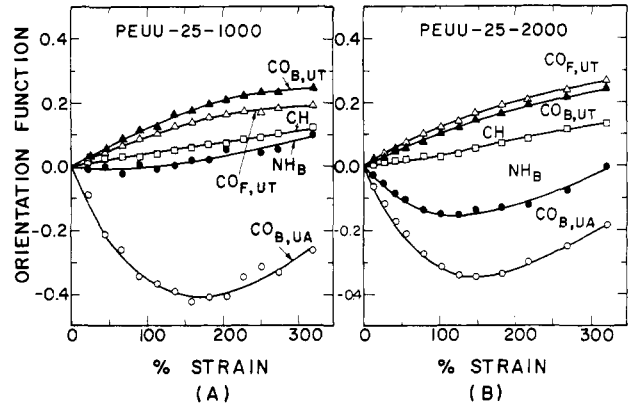

Figure 17. Orientation function vs. elongation curves of (A) PEUU-25-1000 and (B) PEUU-25-2000: (□) CH, (△) $CO_{F,UT}$, (▲) $CO_{B,UT}$, (●) NH_B, (○) $CO_{B,UA}$.

analyzed on the same basis, the data presented in this section are assumed to have semiquantitative significance even though analysis involving peak deconvolution was not applied.

Figure 15 shows the typical relationship between the orientation function (f) and the percent elongation for PEUU samples as represented by the two samples containing 46 wt % hard segment. Upon deformation, the soft segments as monitored by f_{CH} orient into the stretch direction. The orientation behavior of the hard segments is more complicated. A negative value of $f_{CO_{B,UA}}$ or f_{NH_B} indicates that the hard segments within the domains first orient transverse to the stretch direction. In contrast, both the urethane carbonyls orient positively, suggesting that hard segments at the interface become aligned into the stretch direction.

Cooper et al.[30,36] found that when both the soft and hard segments are amorphous, they orient into the stretch direction. The extent of orientation is a function of hard segment content in these amorphous polyurethanes and reflects a change of domain morphology from isolated to interconnected microstructures. With semicrystalline hard segments, their orientation is negative at low elongations but becomes positive at higher elongations. Kimura et al.[14] also found similar orientation behavior of the hard segments in more crystallizable PEUU's that exhibited spherulitic texture.

Bonart[37] proposed a model to describe the deformation mechanism of hard domains in a segmented polyurethane. Upon elongation, local torques, acting through soft segment "force strands", cause the long axis of the hard domains to be oriented in the stretch direction, leading to orientation of the individual hard segment transverse to the stretch direction. Further elongation causes hard segments to slip past one another, breaking up the original structure. As elongation continues, hard segments become progressively more oriented into the stretch direction. It is important to consider whether Bonart's model involving discrete hard domain lamellae is accurate in the first place and also wether the model is applicable to a sample morphology with interconnecting hard domains.

In early studies, Estes et al.[36] proposed a morphological model of polyurethanes having interlocked hard domains. In the unstrained state, the soft segments are essentially in the isotropic random-coil conformation. Urethane segments are, however, aligned approximately perpendicular to the long direction of the hard domains, thereby making the hard domains locally anisotropic. Overall, the hard domains are randomly arranged so that the bulk sample appears mechanically and optically isotropic. In Estes' model the individual hard segments may be initially oriented to different extents depending on the relative orientation of the long dimension of the domain to the stretch direction. The orientation of such an assembly of randomly oriented lamellae gives rise to an average negative orientation of the urethane chain segments since the chain axis is perpendicular to the long axis of the domain. According to Bonart's model, the breakup of hard domains during the elongation should result in a decrease in the fraction of interurethane hydrogen bonding. Such a transition was not detected in measuring $(A_N)_{CO_{B,UA}}$ as a function of elongation. It is suggested that at low strains the deformed PEUU hard segment domains maintain most of their structural integrity and retain the three-dimensional interurea hydrogen bonds. At higher strains some of the lamellae begin to disintegrate, ultimately allowing hard seegment chain orientation parallel to the stretch direction. All this occurs with only a slight decrease in the overall interurea hydrogen bonding. Since the NH_B absorption combines NH groups participating in the interurea, interurethane, or hard to soft segment hydrogen bonding, it is not surprising to observe that the average bonded N–H orientation function (f_{NH_B}) is less negative than the bonded urea carbonyl function ($f_{CO_{B,UA}}$) (Figures 15, 16, and 17).

During the stress relaxation period following sample stretching the orientation of the chain segments will be influenced by molecular relaxation processes. The extent of segmental relaxation will be affected by the relative rigidity of the corresponding phase at the testing temperature (room temperature for this work). Consequently, the strained soft segments having a T_g much lower than

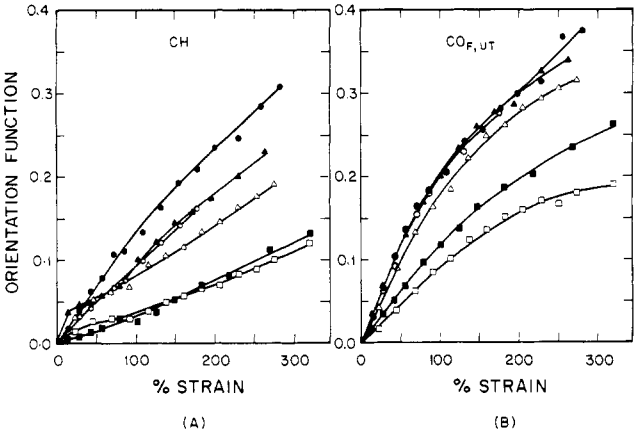

Figure 18. Orientation function vs. elongation curves of (A) CH and (B) $CO_{F,UT}$ of polyether polyurethaneurea samples: (○) PEUU-46-1000, (●) PEUU-46-2000, (△) PEUU-36-1000, (▲) PEUU-36-2000, (□) PEUU-25-1000, (■) PEUU-25-2000.

room temperature tend to disorient toward a more random conformation via an entropy-driven mechanism. The accompanying retractive force exerts a tension on the urethane junctions at the interface between the hard domains and the soft segment matrix; hence they are further aligned into the stretch direction. The hard domains are less affected by the PTMO relaxation, due to their relatively high rigidity. Thus, for each PEUU sample, the soft segment orientation (f_{CH}) was observed to be lower than the orientation of the non-hydrogen-bonded urethanes ($f_{CO_{F,UT}}$).

(2) Soft Segment Orientation Studies. Figure 18 summarizes the soft segment orientation plotted against percent elongation for all the PEUU materials. As the hard segment content and block length were reduced, lower soft segment f values were observed. The storage modulus at room temperature as determined by dynamic mechanical analysis (Figures 6 and 7) also shows a trend consistent with the orientation behavior; i.e., a higher E' *correlates* with higher domain rigidity and less segmental disorientation during the 5-min relaxation period. Both factors result in higher f values.

(3) Hard Segment Orientation Studies. In order to study the influence of block length on segmental orientation, it is instructive to compare IR dichroism results on samples containing similar hard segment concentrations.

The stress hysteresis data showed that PEUU-46 samples contained highly interlocking hard segment domains. However, both the DSC and Rheovibron results also indicated that PEUU-46-2000 had higher phase purity and degree of order in both the hard domains and the polyether matrix phase. Figure 15A,B shows that $f_{CO_{B,UA}}$ and f_{NH_B} of PEUU-46-1000 are less negative than those of PEUU-46-2000. It appears that the hard segment lamellae in the 2000 mol wt sample have better domain cohesion. This arises because PEUU-46-2000 has a higher fraction of urea groups and degree of interurea hydrogen-bonding domain cohesion. Therefore the domains in the longer segment material are not disrupted into microdomains containing bundles of hard segments oriented preferably along the stretch direction until higher strain levels. The elongation at the minimum values of $f_{CO_{B,UA}}$ or f_{NH_B} may serve as a determination of when large scale domain disruption takes place. A higher value of strain at this minimum is observed for PEUU-46-2000 compared to PEUU-46-1000 (140% vs. 100%).

Similar trends of orientation behavior for soft and hard segments within domains or at the interface are observed for sample pairs PEUU-36-1000 and PEUU-36-2000 (Figure 16A,B) and PEUU-25-1000 and PEUU-25-2000 (Figure 18A,B). However, an initially positive f_{NH_B} in PEUU-25-1000 is observed. This arises from the relatively small contribution of the urea linkages to the average hard segment orientation. (PEUU-25-1000 has the lowest urea content (Table I).)

Upon decreasing the hard segment content, a transition of morphology from interconnecting hard and soft segment domains to isolated hard segment domains in a soft segment matrix was suggested by the stress hysteresis results. These isolated hard domains are likely to have a high aspect ratio, however, since a transverse orientation of urea linkages within the hard domains is observed.

The free carbonyls may be located within the polyether phase or in irregular conformations (nonbonded) at the hard domain interface. In both cases hard domain orientation has little influence on the nonbonded urethane carbonyls. In contrast, the regularly packed hydrogen-bonded urethanes are influenced to some extent by hard domain orientation. The above arguments are reflected in a comparison of the orientation behavior of the urethane carbonyls ($f_{CO_{F,UT}}$ and $f_{CO_{B,UT}}$) in samples of PEUU-46-2000 and PEUU-25-1000. As discussed earlier, most of the hard segments of PEUU-46-2000 reside in highly interconnected hard domains that exhibit transverse orientation upon elongation. Consequently, the orientation of hydrogen-bonded urethanes in the interfacial region is affected by these transversely orienting hard segments, leading to a lower value of $f_{CO_{B,UT}}$ than $f_{CO_{F,T}}$. In the case of PEUU-25-1000, the majority of hard segments are located adjacent to relatively small hard segment domains of low urea content. A combination of the influence of a positive hard segment orientation (f_{NH_B}) and less segmental relaxation of the more rigid hydrogen-bonded urethane results in a higher $f_{CO_{B,UT}}$ than $f_{CO_{F,UT}}$ in PEUU-25-1000.

Conclusions

DSC, dynamic mechanical, stress–strain, stress hysteresis, IR peak position, and IR dichroism experiments were carried out to characterize the morphology and properties of polyether polyurethaneureas of systematically varied hard segment content, soft segment molecular weight, and block length.

The PEUU-2000 series samples exhibited a higher degree of phase separation and higher purity of the soft segment phase than the PEUU-1000 series materials. This is reflected by a much lower T_g and higher soft segment crystallization in the PEUU-2000 series. In samples PEUU-25-1000 and PEUU-25-2000, some soft segments appear to be dissolved in the hard domains, which interferes with hard segment packing. This is suggested by the absence of a hard domain melting endotherm and IR frequency shifts of the hydrogen-bonded urea carbonyls.

The mechanical properties were observed to depend primarily on hard segment content and especially on the concentration of urea linkages. This suggests an improvement of hard domain cohesion and an enhanced filler effect through the formation of three-dimensional urea hydrogen bonds in the PEUU materials. Indeed all the PEUU's showed superior high-temperature performance over comparable polyether polyurethanes chain extended with butanediol.

Upon decreasing the hard segment content a transition of morphology from interconnecting hard and soft segment domains to isolated hard segment domains in a soft segment matrix was observed. In PEUU-46-1000 and PEUU-46-2000, deformation of these samples, which contained interlocked domains, resulted in high stress hysteresis and a decrease in concentration of the interurea

hydrogen bonding. IR dichroism measurements were strongly dependent upon the hard domain morphology and the viscoelastic state of the soft segment matrix. The hard segments within domains intially orient transverse to the stretch direction whereas the soft segments orient parallel to the stretch direction. Small differences in the orientation behavior of the hydrogen-bonded and nonbonded urethane units at the hard domain interface were observed for each PEUU sample. These various trends could be interpreted in terms of the slightly different morphology of each sample.

Acknowledgment. We wish to acknowledge partial support of this work by the polymers section of the NSF Division of Materials Research through Grant DMR 81-06888 and by the Naval Air Systems Command through Contract D 00019-81-C033.

Registry No. 4,4'-Methylenebis(phenylene isocyanate)-ethylenediamine-poly(tetramethylene oxide) copolymer, 9053-66-1.

References and Notes

(1) Noshay, A., McGrath, J. E., Eds. "Block Copolymers"; Wiley: New York 1973.
(2) *Adv. Chem. Ser.* **1979**, *No. 176*.
(3) Chang, Y. J. P.; Wilkes, G. L. *J. Polym. Sci., Polym. Phys. Ed.* **1975**, *13*, 455.
(4) Schneider, N. S.; Sung, C. S. P.; Matton, R. W.; Illinger, J. L. *Macromolecules* **1981**, *14*, 212.
(5) Srichatrapimuk, V. W.; Cooper, S. L. *J. Macromol. Sci. Phys.* **1978**, *B15*, 267.
(6) Senich, G. A.; MacKnight, W. J. *Macromolecules* **1980**, *13*, 106.
(7) Bonart, R.; Morbitzer, L.; Muller, E. H. *J. Macromol. Sci. Phys.* **1974**, *B9*, 447.
(8) Sung, C. S. P.; Smith, T. W.; Sung, N. H. *Macromolecules* **1980**, *13*, 117.
(9) Knutson, K.; Lyman, D. J. *Adv. Chem. Ser.* **1982**, *No. 199*.
(10) Sung, C. S. P.; Hu, C. B.; Wu, C. S. *Macromolecules* **1980**, *13*, 111.
(11) Sung, C. S. P.; Hu, C. B. *Macromolecules* **1981**, *14*, 212.
(12) Wilkes, G. L.; Abouzahr, S. *Macromolecules* **1981**, *14*, 458.
(13) Ishihara, H.; Kimura, I.; Saito, K.; Ono, H. *J. Macromol. Sci. Phys.* **1974**, *B10* (*4*), 591.
(14) Kimura, I.; Ishihara, H.; Ono, H.; Yoshihara, N.; Nomura, S.; Kawai, H. *Macromolecules* **1974**, *7*, 355.
(15) Khranovskii, V. A. Dokl. *Akad. Nauk SSSR* **1979**, *244* (2), 408.
(16) Saunders, J. H.; Frisch, K. C. "Polyurethanes, Chemistry and Technology, Part I, Chemistry"; Interscience: New York, 1962.
(17) Koberstein, J. T.; Cooper, S. L.; Shen, M. *Rev. Sci. Instrum.* **1975**, *46*, 1639.
(18) Zbinden, R. "Infrared Spectroscopy of High Polymers", 2nd ed.; Academic Press: New York, 1969.
(19) Siesler, H. W.; Holland-Moritz, K. "Infrared and Raman Spectroscopy of Polymers", Dekker: New York, 1980.
(20) Seymour, R. W.; Estes, G. M.; Cooper, S. L. *Macromolecules* **1970**, *3*, 579.
(21) Hu, C. B.; Ward, R. S., Jr.; Schneider, N. S. *J. Appl. Polym. Sci.*, in press.
(22) Tanaka, A.; Uemura, S.; Ishida, Y. *J. Polym. Sci., Polym. Phys. Ed.* **1972**, *10*, 2093.
(23) Flory, P. J. "Principles of Polymer Chemistry", 9th ed.; Cornell University Press: Ithaca, NY, 1975; p 568.
(24) Flory, P. J. *J. Chem. Phys.* **1949**, *17*, 223; **1947**, *15*, 684.
(25) Paul, D. R; Barlow, J. W.; Bernstein, R. E.; Wahrmund, D. C. *Polym. Sci. Technol.* **1978**, *18*, 1225.
(26) Nishi, T.; Wang, T. T. *Macromolecules* **1975**, *8*, 909.
(27) Nishi, T.; Kwei, T. K. *J. Appl. Polym. Sci.* **1976**, *20*, 1331.
(28) Nielsen, L. E. *Rheol. Acta* **1974**, *13*, 86.
(29) Aggarwal, S. L., Ed. "Block Polymers"; Plenum Press: New York, 1970.
(30) Cooper, S. L.; West, J. S.; Seymour, R. W. "Encyclopedia of Polymer Science and Technology"; Wiley: New York, 1976; Supplementary Volume II, p 521.
(31) Seymour, R. W.; Allegrezza, A. E., Jr.; Cooper, S. L. *Macromolecules* **1973**, *6*, 896.
(32) Seymour, R. W.; Cooper, S. L. *Rubber Chem. Technol.* **1974**, *47*, 19.
(33) Spencer, B. A. MS Thesis, University of Wisconsin, 1978.
(34) Coleman, M. M.; Zarian, J. *J. Polym. Sci., Polym. Phys. Ed.* **1979**, *17*, 837.
(35) Tanaka, T.; Yokoyama, T.; Kaku, K. *Mem. Fac. Sci., Kyushu Univ.* **1963**, *23*, 113.
(36) Estes, G. M.; Seymour, R. W.; Cooper, S. L. *Macromolecules* **1971**, *4*, 452.
(37) Bonart, R. *J. Macromol. Sci. Phys.* **1968**, *B2*, 115.
(38) Seefried, C. G., Jr.; Koleske, J. V.; Critchfield, F. E. *J. Appl. Polym. Sci.* **1975**, *19*, 2493.

^{13}C NMR Study of the Chain Dynamics of Polypropylene and Poly(1-butene) and the Stereochemical Dependence of the Segmental Mobility

Tetsuo Asakura*

Department of Biopolymer Engineering, Faculty of Technology, Tokyo University of Agriculture and Technology, Koganei, Tokyo 184, Japan

Yoshiharu Doi

Department of Chemical Engineering, Faculty of Technology, Tokyo Institute of Technology, Ookayama, Meguro-ku, Tokyo 152, Japan. *Received September 15, 1982*

ABSTRACT: Carbon-13 spin-lattice relaxation times and nuclear Overhauser enhancements of polypropylene and poly(1-butene) have been measured in an *o*-dichlorobenzene-perdeuteriobenzene (9:1 (v/v)) mixture at 50 MHz. The relaxation data for the methine peak of polypropylene, including the 25-MHz data reported previously, were interpreted well in terms of the log χ^2 distribution model of the correlation time. The stereochemical dependence of the spin-lattice relaxation times was also observed for the methine peak of poly(1-butene) as well as polypropylene. The difference is small but significant and tends to be larger when the comparison is done on the correlation times determined with the log χ^2 distribution model. Both the correlation times and the activation energies of poly(1-butene) were considerably larger than those of polypropylene, which indicates that the greater bulkiness of the side group causes higher steric hindrance with the backbone chain.

Introduction

^{13}C NMR has been widely used to examine the chain dynamics of a number of polymers in bulk and solution.[1] One of the most important objectives of these studies is to determine the correlation times for the backbone motion of the polymer. The isotropic rotational diffusion model has been widely applied to describe the polymer motion. Detailed examinations of the relaxation data suggest that

0024-9297/83/2216-0786$01.50/0